Langmuir

ARTICLE

pubs.acs.org/Langmuir

Electrospinning of Polymer-free Nanofibers from Cyclodextrin Inclusion Complexes

Asli Celebioglu and Tamer Uyar*

UNAM-Institute of Materials Science & Nanotechnology, Bilkent University, Ankara 06800, Turkey

ABSTRACT: The electrospinning of polymer-free nanofibers from highly concentrated (160%, w/v) aqueous solutions of hydroxypropyl-β-cyclodextrin (HPβCD) and its inclusion complexes with triclosan (HPβCD/triclosan-IC) was achieved successfully. The dynamic light scattering (DLS) and rheology measurements indicated that the presence of considerable HPβCD aggregates and the high solution viscosity were the key factors in obtaining electrospun HPβCD and HPβCD/triclosan-IC nanofibers without the use of any polymeric carrier. The HPβCD and HPβCD/triclosan-IC solutions containing 20% (w/w) urea yielded no fibers but only beads and splashes because of the depression of the self-aggregation of the HPβCD. The inclusion complexation of triclosan with HPβCD was studied by isothermal titration calorimetry (ITC) and turbidity measurements. The characteristics of the HPβCD and HPβCD/triclosan-IC nanofibers were investigated by Fourier transform infrared spectroscopy (FTIR), thermogravimetric analysis (TGA), X-ray diffraction (XRD), and differential scanning calorimetry (DSC). It was found that the electrospinning of HPβCD/triclosan-IC solution having a 1:1 molar ratio was optimal for obtaining nanofibers without any uncomplexed guest molecules.

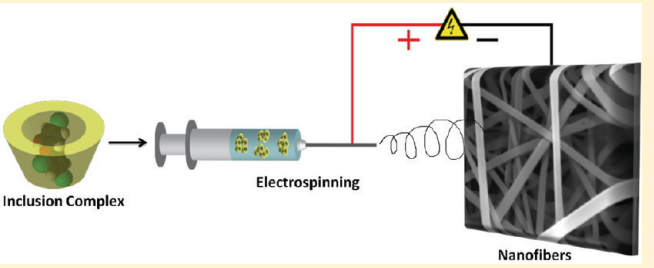

1. INTRODUCTION

Electrospinning has attracted a great amount of attention in the past decade because this cost-effective and versatile technique facilitates the production of functional nanofibers from various polymers, polymer blends, and polymer composites.[1−6] In principle, high-molecular-weight polymers and high polymer concentrations are required for the electrospinning of fibers because polymer chain entanglements and overlapping are very crucial to fiber formation during the electrospinning process.[7,8] Nevertheless, recently it has been demonstrated that microfibers of low-molar-mass gemini surfactant[9] and phospholipid[10] were electrospun because these molecules can form cylindrical micelles that can overlap and entangle in a fashion similar to polymers in their concentrated solutions. Very recently, we have also achieved the electrospinning of methyl-β-cyclodextrin (MβCD) nanofibers without using a polymeric carrier matrix.[11] Cyclodextrins (CDs) are capable of self-assembly and form aggregates via intermolecular interactions such as hydrogen bonding in their solutions.[12−14] The success of the electrospinning of nanofibers from such small molecules is due to the presence of considerable aggregates and reasonable intermolecular interactions between the CD molecules in their concentrated solutions.

CDs are cyclic oligosaccharides having a toroid-shaped molecular structure (Figure 1) that can form noncovalent host−guest inclusion complexes with a variety of molecules including drugs, antibacterials, food additives, textile auxiliaries, and so forth.[15,16] Because the stability, solubility, reactivity, and controlled release of guest molecules can be enhanced by complexation with CD, the cyclodextrin inclusion complexes (CD-IC) are used in various application areas such as pharmaceuticals, functional foods, textiles, sustained/controlled delivery systems, sensors, and many other advanced functional systems.[15−19]

Previously, we have produced electrospun functional polymeric nanofibers containing CDs,[20−22] CD-ICs,[23,24] and CD-pseudopolyrotaxanes.[25] Here, we report on the very first studies on the electrospinning of CD-IC by itself without using a carrier polymer matrix. In this study, we achieved the electrospinning of polymer-free nanofibers from hydroxypropyl-β-cyclodextrin (HPβCD) and its inclusion complexes with triclosan (HPβCD/triclosan-IC). We anticipated that the electrospinning of nanofibers from CD-ICs would be particularly attractive because of the exclusive properties obtained by combining the very large surface area of nanofibers/nanowebs with specific functionality of the CD-ICs.

2. EXPERIMENTAL SECTION

Materials. Triclosan (>%97 (HPLC), Sigma, Germany) and urea (>%99.5, Merck, Germany) were purchased commercially. The water used was from a Millipore Milli-Q ultrapure water system. The HPβCD was obtained from Wacker Chemie AG (Germany). The materials were used without any purification.

Preparation of HPβCD and HPβCD/Triclosan-IC Solutions. The formation of HPβCD/triclosan-IC was achieved in aqueous solution by using a 1:1 molar ratio of HPβCD/triclosan. Additionally, we

Received: December 19, 2010
Revised: March 18, 2011
Published: April 22, 2011

dx.doi.org/10.1021/la1050223 | *Langmuir* 2011, 27, 6218–6226

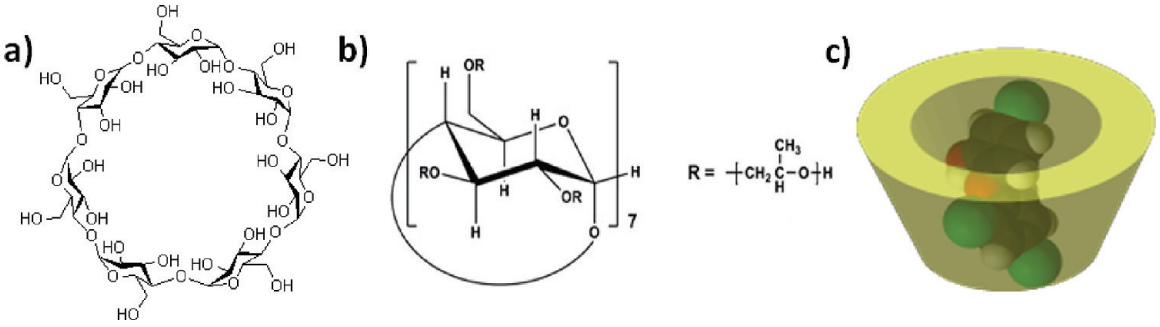

Figure 1. Chemical structure of (a) β-CD and (b) HPβCD. (c) Schematic representation of the cyclodextrin/triclosan inclusion complex.

have also prepared HPβCD/triclosan-IC containing a higher amount of a guest molecule: HPβCD/triclosan having 1:1.3 mol ratio. For HPβCD/triclosan-IC, first triclosan was put in water and stirred at 40 °C for 0.5 h. Because triclosan is not water-soluble, we obtained a dispersion. Then, HPβCD (160%, w/v) was added to the triclosan solution, and the solution became clear after stirring for 0.5 h at 40 °C because of the dissolution of triclosan by forming an inclusion complex with HPβCD. As the solution was cooled down and stirred overnight at room temperature, a white, highly turbid HPβCD/triclosan-IC solution was obtained. However, a homogeneous, clear aqueous solution of HPβCD was prepared by dissolving HPβCD (160%, w/v) in water by stirring for 1 h at 50 °C; thereafter, it was cooled to room temperature before electrospinning. The clear HPβCD solution and the turbid HPβCD/triclosan-IC solutions having 1:1 and 1:1.3 molar ratios were electrospun. For comparison, a physical mixture of HPβCD/triclosan was prepared in the solid state by grinding HPβCD nanofibers and triclosan in an agar mortar for 15 min by using an identical molar ratio (1:1).

Electrospinning. The clear solution of HPβCD and the turbid solutions of HPβCD/triclosan-IC were placed in a 1 mL syringe fitted with a metallic needle of 0.45 mm inner diameter. The syringe was fixed horizontally on the syringe pump (model SP 101IZ, WPI, USA). The electrode of the high-voltage power supply (Matsusada Precision, AU Series, Japan) was clamped to the metal needle tip, and the cylindrical aluminum collector was grounded. The feed rate of solutions was 0.5 mL/h, the applied voltage was 15 kV, and the tip-to-collector distance was kept at 10 cm. Electrospun nanofibers were deposited on a grounded stationary cylindrical metal collector covered with a piece of aluminum foil. The electrospinning apparatus was enclosed in a Plexiglas box, and electrospinning was carried out at 24 °C at 45% relative humidity. The collected nanofibers were dried at room temperature under the fume hood overnight and stored several days before their analyses.

Measurements and Characterization. A Nano-ZS Zetasizer dynamic light scattering (DLS) system (Malvern Instruments, U.K.) was used to measure the particle size of the aggregates in HPβCD solutions.

A rheometer (Anton Paar Physica MCR 301, Austria) equipped with a cone/plate accessory (spindle type CP40-2) was used to measure the rheological behavior of the HPβCD and HPβCD/triclosan-IC solutions in the range of 0.1 to 100 Pa with shear stress at 22 °C.

The isothermal titration experiment was performed by using isothermal titration calorimetry (ITC) (ITC200 Microcalorimeter, France), and the data were analyzed with Origin software. Water was used as the solvent system for both HPβCD and triclosan. A 0.025 mM triclosan dispersion was prepared and sonicated for 15 min. While the reaction cell was filled with 200 μL of triclosan solution, the syringe was filled with 40 μL of the HPβCD solution (0.25 mM). The experiment was carried out at 25 °C by titrating (1 μL/injection, 40 injections total) the HPβCD solution into the triclosan solution. The reference cell was charged with 150 μL of deionized water, and the system was stirred at 500 rpm during the titration. To attain thermal equilibrium between each titration, 200 s time intervals were applied.

A UV−vis−NIR spectrophotometer (Varian Cary 5000, USA) was used in the wavelength range of 400−800 nm to observe the absorbance differentiation as the HPβCD/triclosan-IC solution became turbid in the progressing time interval. For this, the HPβCD/triclosan-IC (1:1) solution was prepared and the absorption measurements were taken after 1, 3, 6, 9, 12, and 15 h.

The analyses of the collected nanofibers were carried out after several days of their production. A scanning electron microscope (SEM) (FEI−Quanta 200 FEG, Netherlands) was used for the morphological investigation of the electrospun nanofibers. Samples were sputtered with 7 nm Au/Pd prior to SEM imaging. The average fiber diameter (AFD) was determined from the SEM images, and around 100 fibers were analyzed.

The X-ray diffraction (XRD) (PANalytical X'Pert powder diffractometer, Netherlands) data of the HPβCD, HPβCD/triclosan-IC nanofibers and the physical mixture of HPβCD/triclosan were recorded by using Cu Kα radiation in a range of 2θ = 5−30°.

Differential scanning calorimetry (DSC) (TA Q2000, USA) and thermogravimetric analysis (TGA) (TA Q500, USA) were used for the investigation of the thermal properties of the samples. DSC analyses were carried out under N_2; initially, samples were equilibrated at −90 °C and then heated to 300 °C at a heating rate of 10 °C/min. The TGA of the samples was carried out from 25 to 500 °C at a 20 °C/min heating rate, and N_2 was used as a purge gas.

The infrared spectra of the samples were obtained by using a Fourier transform infrared spectrometer (FTIR) (Bruker-VERTEX 70, Germany). The samples were mixed with potassium bromide (KBr) and pressed as pellets. The scans (64 scans) were recorded between 4000 and 400 cm^{-1} at a resolution of 4 cm^{-1}.

3. RESULTS AND DISCUSSION

Electrospinning of HPβCD Nanofibers. β-CD has very limited water solubility,[26] yet the chemical modification of β-CD by random substitution of the hydroxyl groups of CD with hydroxypropyl groups resulted in amorphous HPβCD having much higher aqueous solubility compared to that of native β-CD.[27] Here, we prepared clear aqueous solutions of HPβCD having very high concentrations (100, 120, 140, and 160%, w/v) for the electrospinning of HPβCD nanofibers without using a polymeric carrier. At lower HPβCD concentrations (100−140%, w/v), beads and beaded nanofibers were obtained. However, at 160% (w/v) concentration, bead-free uniform HPβCD nanofibers (Figure 2a) were produced with fiber diameters in the range of 200−1600 nm having an average fiber diameter of 745 ± 370 nm (Figure 2b and Table 1).

We have investigated the characteristics of the concentrated HPβCD solutions by DLS and rheology measurements in order

dx.doi.org/10.1021/la1050223 |*Langmuir* 2011, 27, 6218–6226

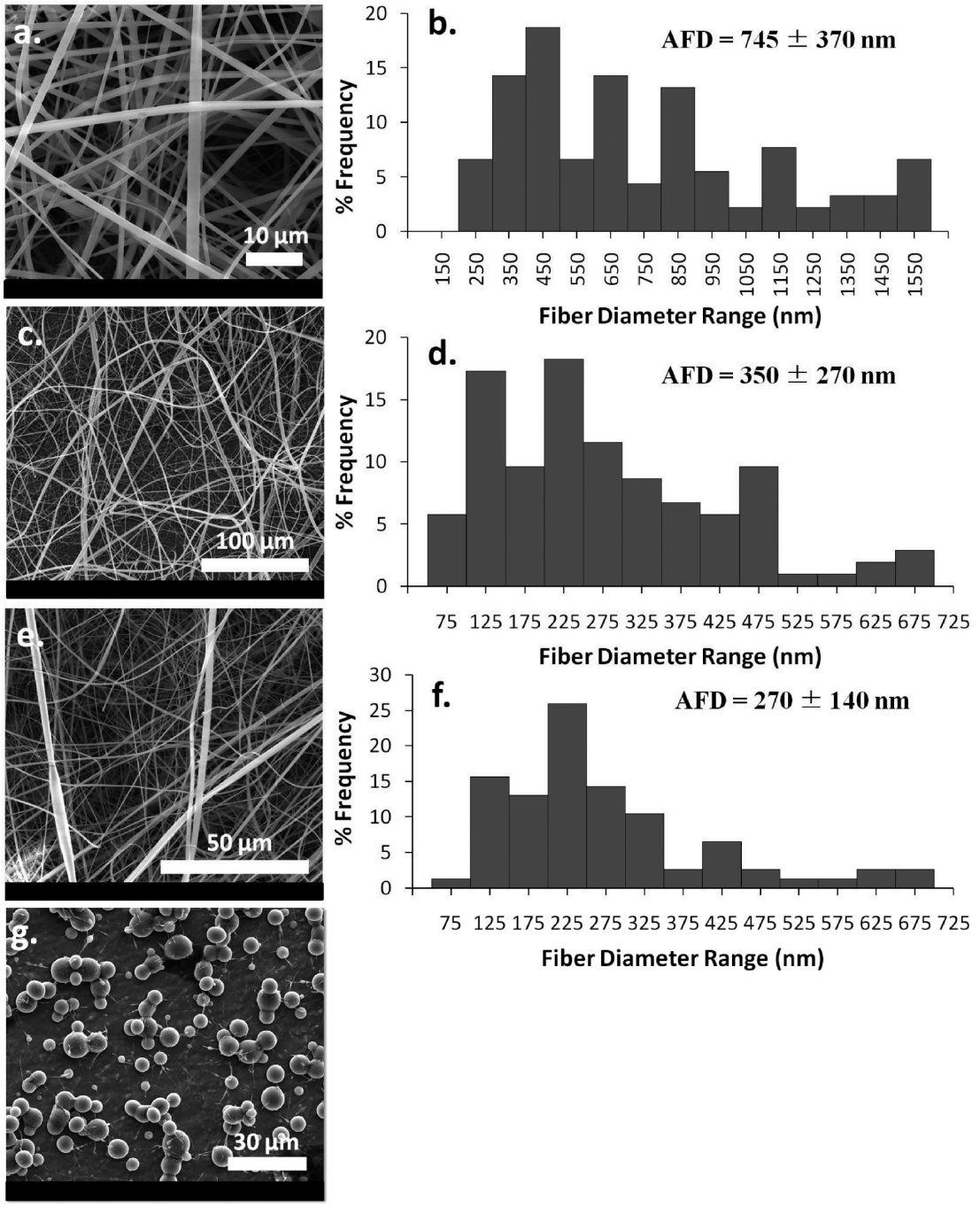

Figure 2. Representative SEM image of (a) HPβCD nanofibers obtained from a 160% (w/v) HPβCD solution and (b) the fiber diameter distribution. SEM images of HPβCD nanofibers containing (c) 5 and (e) 10% (w/w) urea and (d, f) their fiber diameter distributions, respectively. (g) SEM image of bead structures obtained from 160% (w/v) HPβCD containing 20% (w/w) urea.

to understand the electrospinnability of HPβCD by itself. Studies have shown that CDs are capable of self-assembly and form aggregates via intermolecular interactions in their concentrated solutions.[12−14] Here, the DLS measurements revealed the presence of self-aggregated HPβCD molecules in their concentrated solutions (Figure 3a and Table 2). The size of the aggregates was measured to be around 6.5 nm with a polydispersity index (PDI) of 0.26 for 100% (w/v) HPβCD solution. At 120 and 140% (w/v) HPβCD solutions, the size of the aggregates increased to 7.0 nm (PDI = 0.32) and 8.0 nm (PDI = 0.35), respectively. The size of the aggregates reached 9.2 nm (PDI = 0.40) for a 160% (w/v) HPβCD solution. The DLS measurements clearly showed that the size of the HPβCD aggregates was increased and the particle size distribution became broader as the concentration of the HPβCD solution increased from 100 to 160% (w/v).

Rheological measurements for HPβCD and HPβCD/triclosan-IC solutions were also performed. HPβCD and HPβCD/triclosan-IC solutions showed Newtonian behavior, as seen from the rheology data (Figure 4). A significant increase in the viscosity of the HPβCD solutions was recorded as the concentration of

dx.doi.org/10.1021/la1050223 |*Langmuir* 2011, 27, 6218–6226

Table 1. Morphological Findings of the Resulting Electrospun Nanofibers Obtained from HPβCD and HPβCD/Triclosan-IC Solutions

solution	urea (%, w/w)	fiber morphology	fiber diameter range (nm)	average fiber diameter (nm)
HPβCD		bead-free nanofibers	200−1600	745 ± 370
HPβCD	5	bead-free nanofibers	50−700	350 ± 270
HPβCD	10	bead-free nanofibers	50−700	270 ± 140
HPβCD	20	no fiber formation		
HPβCD/triclosan-IC (1:1)		bead-free nanofibers	200−900	570 ± 130
HPβCD/triclosan-IC (1:1.3)		bead-free nanofibers	50−900	380 ± 200
HPβCD/triclosan-IC (1:1)	20	no fiber formation		

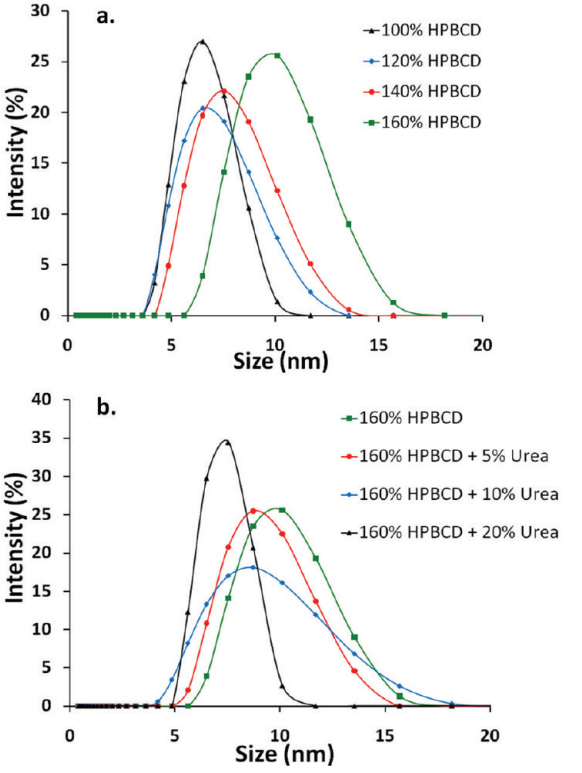

Figure 3. Size distribution of HPβCD aggregates for (a) 100, 120, 140, and 160% (w/v) HPβCD concentrations and for (b) 160% (w/v) HPβCD concentration including 5, 10, and 20% (w/w) urea.

HPβCD increased from 100 to 160% (w/v). The DLS and rheology data are in good agreement with each other, and higher solution viscosity was possibly due to the higher number of HPβCD aggregates and their growing sizes in their concentrated solutions.

At lower HPβCD concentrations (100−140%, w/v), the electrospinning of uniform HPβCD nanofibers was not achieved possibly because of the insufficient number of HPβCD aggregates and their smaller particle size that resulted in the destabilization of the electrified jet during electrospinning. This behavior is typically observed for polymer solutions having lower concentrations and electrospinning yield beads and/or beaded nanofibers because of the lack of sufficient polymer chain entanglements and overlapping.[1,8,28] At 160% (w/v) HPβCD concentration, SEM findings suggested that full stretching of the electrified jet was achieved because of the high solution viscosity and the presence of a considerable number of HPβCD aggregates; therefore, bead-free HPβCD nanofibers were obtained.

Table 2. DLS Measurements of HPβCD Solutions at 25 °C (Equilibrium at 25 °C for 2 Minutes Prior to Measurement) Summarizing the Average Diameter (nm) and Polydispersity Index (PDI) of HPβCD Aggregates

sample	intensity-average diameter (d, nm)	PDI
100% HPβCD	6.5	0.26
120% HPβCD	7.0	0.32
140% HPβCD	8.0	0.35
160% HPβCD	9.2	0.40
160% HPβCD + 5% urea	9.1	0.36
160% HPβCD + 10% urea	9.0	0.48
160% HPβCD + 20% urea	8.1	0.28

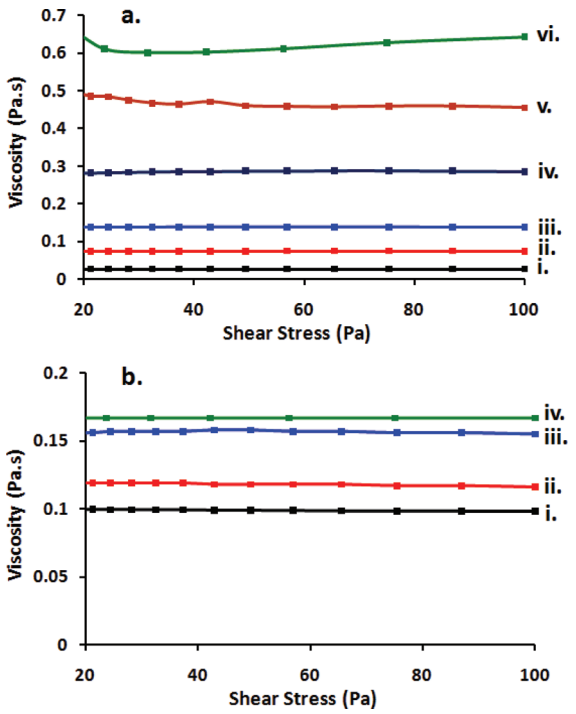

Figure 4. Steady shear viscosity of (a, i) 100, (ii) 120, (iii) 140, and (iv) 160% (w/v) HPβCD solution, (v) HPβCD/triclosan-IC (1:1.3), and (vi) HPβCD/triclosan-IC (1:1) solutions. (b) 160% (w/v) HPβCD solution containing (i) 20, (ii) 10, and (iii) 5% (w/w) urea and (iv) a HPβCD/triclosan-IC (1:1) solution containing 20% (w/w) urea.

It is known that the addition of urea breaks the hydrogen bonds between CD molecules and therefore causes a notable

dx.doi.org/10.1021/la1050223 |*Langmuir* 2011, 27, 6218–6226

depression of the self-association of the CD molecules in water.[29,30] Here, we added urea (5, 10, and 20% (w/w) with respect to HPβCD) to the 160% (w/v) HPβCD aqueous solution. We observed that the size of the aggregates got smaller (Figure 3b and Table 2) and the viscosity of the HPβCD solution decreased as the urea content increased from 5 to 20% (w/w) (Figure 4b). The electrospinning of a 160% (w/v) HPβCD aqueous solution containing 5 and 10% (w/w) urea yielded thinner nanofibers (Figure 2c,e) in the range of 50−700 nm having average fiber diameters of 350 ± 270 and 270 ± 140 nm, respectively (Figure 2d,f). The urea (5 and 10%, w/w)-containing HPβCD solutions yielded thinner fibers possibly because of the low viscosity of the solutions; therefore, the jet was subjected to more stretching during electrospinning. This behavior is very typical for the electrospinning of polymer solutions having a low viscosity which resulted in thinner fibers when electrospun.[1,28] In the case of an HPβCD aqueous solution containing 20% (w/w) urea, no fibers were yielded, only beads (Figure 2g), because the breakup of the electrospinning jet occurred, which was possibly due to the absence of a sufficient number of HPβCD aggregates and the low viscosity of the solution. These results showed that the success of the electrospinning of HPβCD nanofibers without the need of any polymeric carrier is due to the presence of a considerable number of aggregates and reasonable intermolecular interactions between the HPβCD molecules in their concentrated solutions.

Electrospinning of HPβCD/Triclosan-IC Nanofibers. Studies have shown that triclosan can form inclusion complexes with different types of cyclodextrins including β-CD,[31,32] HPβCD,[33] and MβCD.[33] Here, we have studied the inclusion complexation of triclosan with HPβCD by using ITC. ITC is a powerful and highly sensitive technique for studying the interactions between the guest molecules and the host molecules in the CD-IC systems.[34,35] ITC measurements give thermodynamic and kinetic information as well as the molar stoichiometry of the CD-ICs. The ITC analyses (Figure 5, Table 3) indicated that the standard formation enthalpy (ΔH°) of the inclusion complexion between HPβCD and triclosan was -521 ± 9 kJ mol^{-1}, signifying that the complex formation is an exothermic processes. In addition, the negative nature of enthalpy changes indicated that the inclusion complexation process is enthalpy-driven.[34] The entropy effect ($T\Delta S$) was also negative, so the complexation between HPβCD and triclosan is entropically unfavorable.[34] The high value of the association constant ($K_s = (9.6 \pm 4.2) \times 10^6$ M^{-1}) suggested strong host−guest interactions. Moreover, the stoichiometry of the complexation between HPβCD and triclosan was calculated to be ∼1:1 mol/mol from the ITC data ($N = 0.98$).

The inclusion complexation of triclosan with highly concentrated HPβCD (160%, w/v) was also studied visually and by

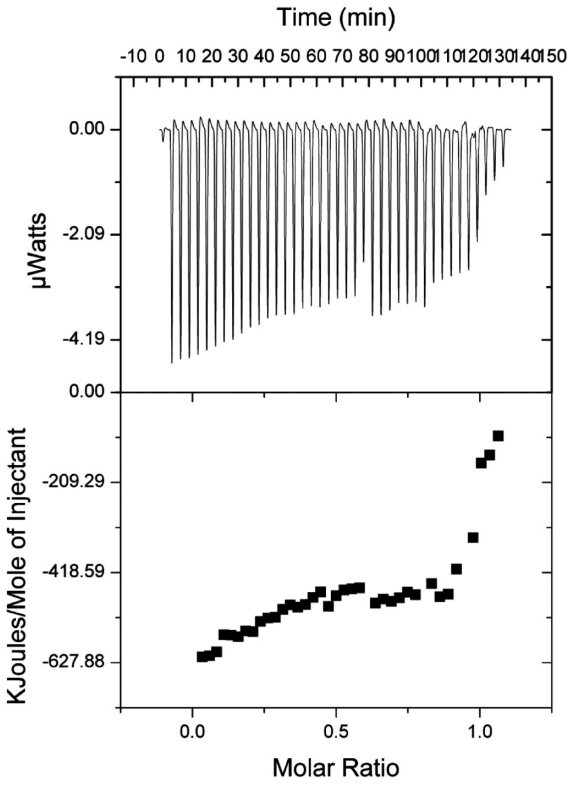

Figure 5. Isothermal calorimetric titration of triclosan with HPβCD in water at 25 °C: (upper) raw data for 40 injections of HPβCD solution into triclosan solution; (lower) titration curve obtained from the integration of the calorimetric traces.

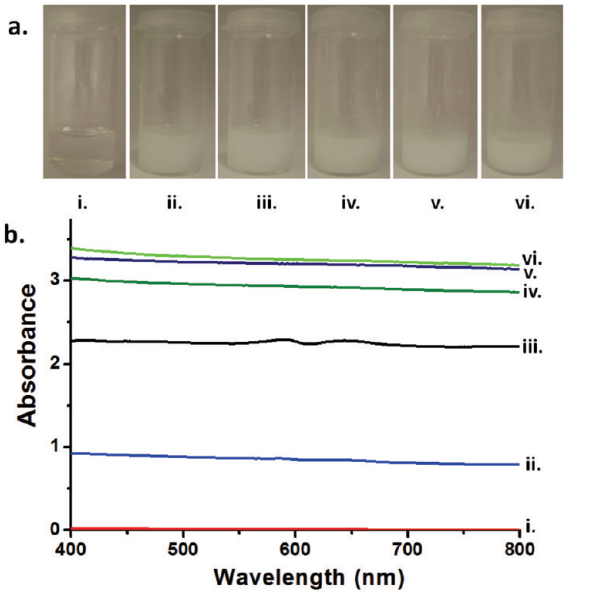

Figure 6. (a) Visual observation of a HβCD/triclosan-IC (1:1 molar ratio) solution after mixing of the two components for (i) 1, (ii) 3, (iii) 6, (iv) 9, (v) 12, and (vi) 15 h. (b) UV−vis spectrum of the same HβCD/triclosan (1:1 molar ratio) solution after (i) 1, (ii) 3, (iii) 6, (iv) 9, (v) 12, and (vi) 15 h.

Table 3. Thermodynamic Parameters Obtained from ITC Measurements[a]

triclosan (mM)	HPβCD (mM)	N	K_s (M^{-1}) × 10^6	ΔH°(kJ/mol)	$T\Delta S^\circ$ (kJ/mol)
0.025	0.25	0.98	9.6 ± 4.2	−521 ± 9	−478

[a] Stoichiometry (N), complex stability constants (K_s/M^{-1}), standard enthalpy changes (ΔH°/kJ mol^{-1}), and entropy changes ($T\Delta S^\circ$/kJ mol^{-1}) for inclusion complexation of the triclosan with HPβCD in water at 298 K.

dx.doi.org/10.1021/la1050223 |*Langmuir* 2011, 27, 6218–6226

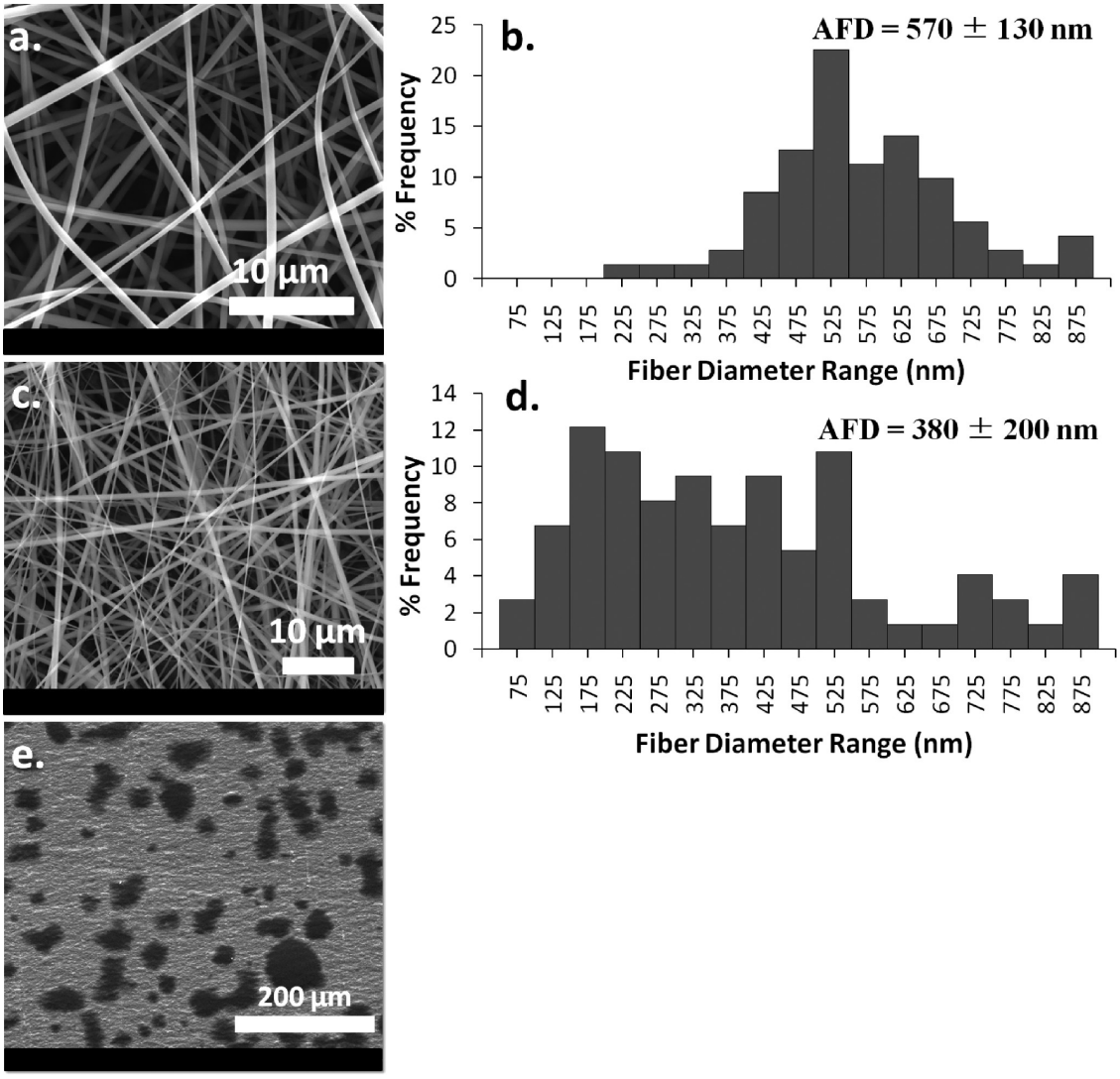

Figure 7. Representative SEM images and fiber diameter distribution of the electrospun nanofibers obtained from (a, b) a 160% (w/v) HPβCD/triclosan-IC (1:1) solution and (c, d) a 160% (w/v) HPβCD/triclosan-IC (1:1.3) solution, respectively. (e) SEM image of the splashed area obtained from a 160% (w/v) HPβCD/triclosan-IC (1:1) solution containing 20% (w/w) urea.

turbidity measurements performed with a UV−vis spectrometer (Figure 6). Triclosan is insoluble in water and forms a dispersion; however, when 160% (w/v) HPβCD was added, the solution became clear and transparent because triclosan become water-soluble as a result of the inclusion complexation with HPβCD (Figure 6a.i). Because the mixing continued for a longer time (1−15 h), the solution became very turbid because of the aggregation of HPβCD/triclosan-IC (Figure 6a, ii−vi). Figure 6b clearly shows the increasing absorbance values as a function of time for the HPβCD/triclosan-IC solution as the solution became more turbid. This behavior is typically observed for CD-IC systems as the solubility of CD decreased substantially when complexed with guest molecules and therefore results in very turbid solutions.[33,36,37]

We have prepared HPβCD/triclosan-IC solutions having two different stoichiometries, that is, HPβCD/triclosan having a 1:1 molar ratio and one containing a greater number of guest molecules: HPβCD/triclosan having a 1:1.3 molar ratio. These turbid HPβCD/triclosan-IC solutions were electrospun into nanofibers by themselves without the addition of any carrier polymeric matrix. The representative SEM images and fiber diameter distributions of the electrospun HPβCD/triclosan-IC nanofibers are displayed in Figure 7. Bead-free nanofibers of HPβCD/triclosan-IC (1:1 molar ratio) (Figure 7a) were obtained with diameters in the range of 200−900 nm having an average fiber diameter of 570 ± 130 nm (Figure 7b). In the case of HPβCD/triclosan-IC (1:1.3 molar ratio), the bead-free nanofibers (Figure 7c) within the range of 50−900 nm having an average fiber diameter of 380 ± 200 nm were obtained (Figure 7d). The HPβCD/triclosan-IC nanofibers having a 1:1.3 molar ratio were thinner when compared to those having a 1:1 molar ratio owing to the low solution viscosity (Figure 4a, v−vi) and therefore were subjected to more stretching during electrospinning. Unfortunately, we were not able to perform the DLS measurements because of the turbid nature of the HPβCD/triclosan-IC solutions; therefore, the size of the aggregates could not be measured. However, the viscosity of the HPβCD/triclosan-IC solutions was measured to be higher

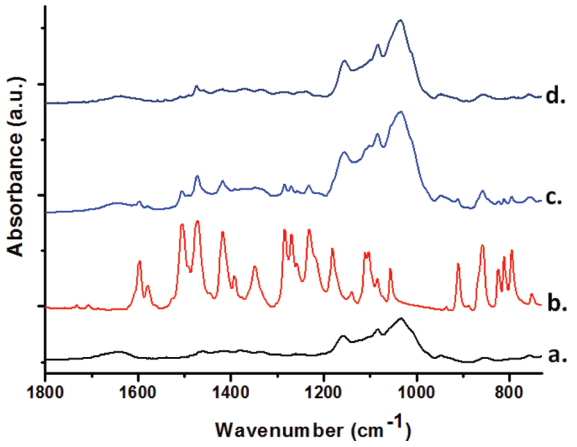

Figure 8. FTIR spectra of (a) HPβCD nanofibers, (b) pure triclosan, (c) a HPβCD/triclosan (1:1 molar ratio) physical mixture, and (d) HPβCD/triclosan-IC (1:1 molar ratio) nanofibers.

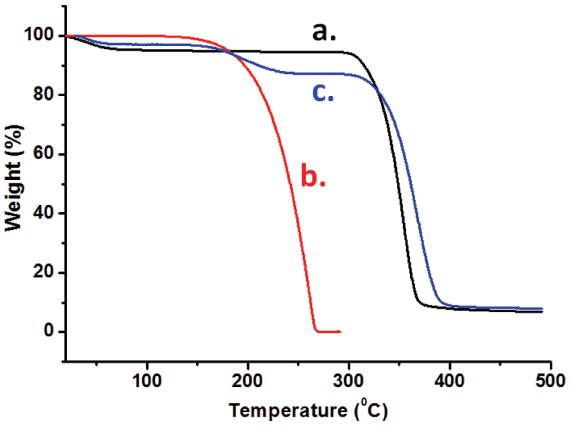

Figure 9. TGA thermograms of (a) HPβCD nanofibers, (b) pure triclosan, and (c) HPβCD/triclosan-IC nanofibers (1:1 molar ratio).

than that of the HPβCD solution (Figure 4a, iv–vi), suggesting that a considerable number of aggregates were present in HPβCD/triclosan-IC solutions and therefore resulted in bead-free nanofibers when electrospun. Similar to HPβCD solution, the addition of 20% (w/w) urea to HPβCD/triclosan-IC lowered the solution viscosity (Figure 4b, iv) and splashes were obtained instead of fibers (Figure 7e), indicating that the urea disrupted the HPβCD aggregates and therefore the breakup in the electrospinning jet was inevitable.

Characterization of HPβCD and HPβCD/Triclosan-IC Nanofibers. The characterizations of the HPβCD and HPβCD/triclosan-IC nanofibers were carried out by FTIR, TGA, XRD, and DSC. Pure triclosan and the physical mixture of HPβCD nanofibers with triclosan were also analyzed for comparison.

The FTIR spectra of pure triclosan, HPβCD nanofibers, a HPβCD/triclosan physical mixture, and HPβCD/triclosan-IC nanofibers are depicted in Figure 8. In the FTIR spectrum of the HPβCD nanofibers (Figure 8a), the salient absorption bands at around 1020 and 1070 cm^{-1} correspond to the coupled C–C and C–O stretching vibrations, and the absorption band at around 1150 cm^{-1} is attributed to the antisymmetric stretching vibration of the C–O–C glycosidic bridge. The FTIR spectrum of pure triclosan (Figure 8b) exhibited characteristic peaks at 1598, 1579, 1507, 1471, 1417, and 1392 cm^{-1} corresponding to vibrations involving C–C stretching inside the benzene ring.[32] The peaks in the region from 1300 to 1000 and 900 to 750 cm^{-1} are due to in-plane and out-of-plane bending of the aromatic ring C–H bonds, respectively.[32] For the HPβCD/triclosan physical mixture, the characteristic peaks for both HPβCD and triclosan were present without any shifts in the absorption bands (Figure 8c). However, in the case of HPβCD/triclosan-IC nanofibers, characteristic bands of triclosan such as those at 1471 and 1417 cm^{-1} shifted to 1474 and 1420 cm^{-1}, respectively (Figure 8d), suggesting the host–guest interactions between HPβCD and triclosan in the electrospun nanofibers. Similar peak shifts were also reported in the literature for CD/triclosan inclusion complexes.[38] In addition, the characteristic peaks of triclosan were suppressed in HPβCD/triclosan-IC nanofibers when compared to those of its physical mixture. The attenuation of the absorption bands of guest molecules are typically observed for the CD-IC systems because the inclusion of guest molecules in the CD cavity hinder their molecular vibrations; therefore, the intensity of their absorption bands is diminished.[38,39] In brief, the shifts in the characteristic bands of triclosan and their attenuation suggested strong host–guest interactions in HPβCD/triclosan-IC nanofibers.

TGA thermograms of pure triclosan, HPβCD nanofibers, and HPβCD/triclosan-IC nanofibers are given in Figure 9. The TGA curve of HPβCD nanofibers showed two weight losses: the initial weight loss below 100 °C was due to water loss, and the major weight loss above 300 °C corresponded to the main thermal degradation of HPβCD (Figure 9a). In the case of HPβCD/triclosan-IC nanofibers, three weight losses were observed: the water loss below 100 °C, the second weight loss between 150 and 250 °C that was due to the evaporation/degradation of triclosan, and the main degradation of HPβCD above 300 °C (Figure 9c). From the TGA data, the amount of triclosan was calculated to be ~10% (w/w, with respect to HPβCD) in the HPβCD/triclosan-IC nanofibers that correspond to 1:1 molar ratio complexation between HPβCD and triclosan. The TGA data correlates with the ITC data, and 1:1 complexation between HPβCD and triclosan was obtained from ITC measurements. The TGA findings also indicate that the initial amount of triclosan was preserved and no loss of guest molecules has occurred during the electrospinning process. The preservation of triclosan during electrospinning is also evidence of its complexation with HPβCD because its stability was sustained against evaporation. For instance, we previously observed that an additive such as menthol without a CD complex could not be preserved during the electrospinning process of the polystyrene/menthol mixture.[24] In the case of complexation, the water molecules inside the CD cavity are displaced by the guest molecules. In addition, the temperature stability of a volatile guest molecule would increase because of the interaction with the CD cavity.[39–41] HPβCD/triclosan-IC nanofibers have minimal water content when compared to HPβCD nanofibers. Moreover, TGA of HPβCD/triclosan-IC nanofibers showed that the thermal degradation temperature (T_d) of triclosan has slightly shifted to higher temperature (T_d onset at ~150 °C) when compared to that of pure triclosan (T_d onset at ~140 °C). In short, the TGA findings suggested that triclosan was in the complexed state with HPβCD in the nanofibers.

The XRD patterns of the HPβCD/triclosan-IC nanofibers are very similar to those of pure HPβCD nanofibers having amorphous structures (Figure 10). In the CD-ICs, the guest molecules

dx.doi.org/10.1021/la1050223 |*Langmuir* 2011, 27, 6218–6226

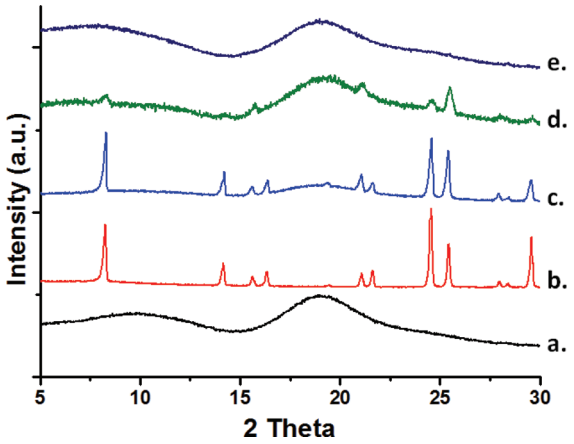

Figure 10. XRD patterns of (a) HPβCD nanofibers, (b) pure triclosan, (c) HβCD/triclosan (1:1 molar ratio) physical mixture, (d) HPβCD/triclosan-IC nanofibers (1:1.3 molar ratio), and (e) HPβCD/triclosan-IC nanofibers (1:1 molar ratio).

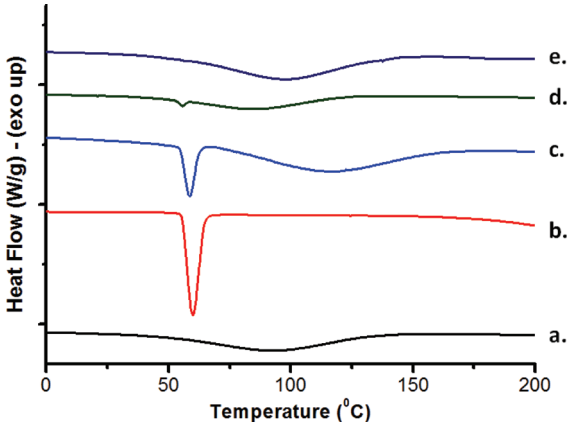

Figure 11. DSC thermograms of (a) HPβCD nanofibers, (b) pure triclosan, (c) a HβCD/triclosan (1:1 molar ratio) physical mixture, (d) a HPβCD/triclosan-IC nanofibers (1:1.3 molar ratio), and (e) HPβCD/triclosan-IC nanofibers (1:1 molar ratio).

are isolated from each other by the CD cavities; therefore, they cannot form crystals.[40] The XRD of HPβCD/triclosan-IC nanofibers (Figure 10e) has shown no diffraction pattern for triclosan, suggesting that the triclosan molecules were included inside the HPβCD cavity. However, the physical mixture of HPβCD/triclosan has diffraction peaks for uncomplexed triclosan (Figure 10c).

DSC is a useful technique for determine whether the guest molecules are included inside the CD cavities.[39,40] A thermal transition such as the melting point (T_m) for guest molecules would be observed if there are any free uncomplexed guest molecules present in the CD-IC system. DSC scans of pure triclosan (Figure 11b) and the physical mixture of HPβCD/triclosan (Figure 11c) exhibited a melting point for triclosan at around 60 °C whereas no melting point was observed for the HPβCD/triclosan-IC (1:1) nanofibers (Figure 11e), suggesting that the triclosan molecules were included inside the HPβCD cavity. In short, the absence of a thermal event such as T_m for guest molecules in HPβCD/triclosan-IC nanofibers is evidence of true inclusion complexation.

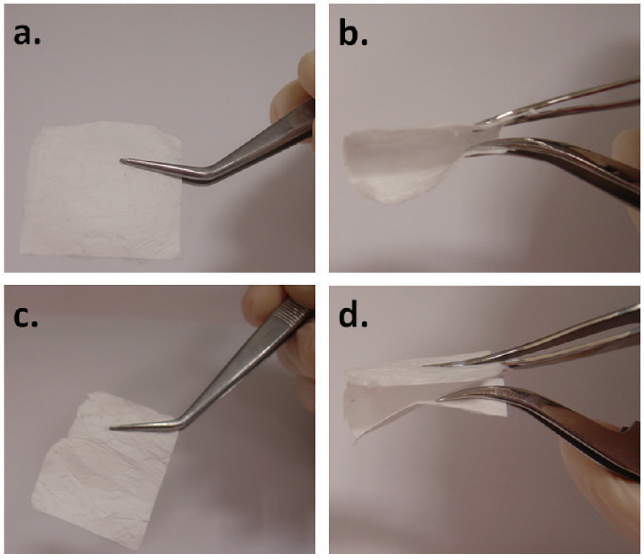

Figure 12. Photographs showing that the nanofibrous webs have mechanical integrity and can be easily handled and folded as a free-standing web. (a, b) HPβCD nanoweb. (c, d) HPβCD/triclosan-IC (1:1 molar ratio) nanoweb.

The XRD of HPβCD/triclosan-IC (1:1.3 molar ratio) nanofibers has shown diffraction peaks (Figure 10d), and the DSC scan exhibited a melting point at around 60 °C (Figure 11d) that is due to the presence of some uncomplexed triclosan molecules. These findings suggest that the electrospinning of nanofibers from HPβCD/triclosan-IC having a 1:1 molar ratio is optimal for obtaining HPβCD-IC nanofibers without any free guest molecules.[31,42] This also correlates with ITC and TGA findings as discussed previously.

The mechanical integrity of HPβCD and HPβCD/triclosan-IC nanofibrous webs was tested qualitatively. Compared to electrospun polymeric nanowebs, they were expected to be weak because they are made of amorphous small molecules. Nevertheless, our observations indicated that these HPβCD and HPβCD/triclosan-IC nanofibrous webs have some mechanical integrity and they can be easily handled and folded as a free-standing web (Figure 12).

4. CONCLUSIONS

The electrospinning of nanofibers from CD-IC is quite challenging because it is a nonpolymeric system. At the same time, electrospun CD-IC nanofibers would be very intriguing because of the exclusive properties obtained by the very large surface area of the nanofibers along with specific functionalities of CD-IC supramolecular structures. In this study, we report the first results on the electrospinning of nanofibers from CD-IC without the use of any polymeric carrier. A widely used antibacterial agent (triclosan) was complexed with HPβCD and then electrospun into uniform nanofibers. DLS and rheology measurements elucidated that bead-free nanofibers of HPβCD and HPβCD/triclosan-IC were able to be electrospun because of the presence of sufficient aggregates and intermolecular interactions between the HPβCD molecules in their highly concentrated (160%, w/v) aqueous solutions. The addition of 20% (w/w) urea to HPβCD and HPβCD/triclosan-IC solutions resulted in the depression of the self-aggregation of the HPβCD molecules;

dx.doi.org/10.1021/la1050223 |*Langmuir* 2011, 27, 6218–6226

therefore, these solutions yielded no fibers but only beads and splashes when electrospun. The FTIR, TGA, XRD, and DSC analyses suggested the presence of a host−guest interaction between triclosan and HPβCD in the electrospun nanofibers. It was found that having 1:1 host−guest complexation was optimal for HPβCD/triclosan-IC nanofibers without any free guest molecules. We are currently investigating the stability, release profile, and antibacterial properties of HPβCD/triclosan-IC nanofibers.

AUTHOR INFORMATION

Corresponding Author

*E-mail: tamer@unam.bilkent.edu.tr. Phone: (+90)3122903571. Fax: (+90)3122664365.

ACKNOWLEDGMENT

The State Planning Organization (DPT) of Turkey is acknowledged for the support of UNAM-Institute of Materials Science & Nanotechnology. T.U. acknowledges EU FP7-PEOPLE-2009-RG Marie Curie-IRG for funding the NANOWEB (PIRG06-GA-2009-256428) project. A.C. acknowledges TUBITAK-BIDEB for the national graduate study scholarship.

REFERENCES

(1) Ramakrishna, S.; Fujihara, K.; Teo, W.; Lim, T.; Ma, Z. *An Introduction to Electrospinning and Nanofibers*; World Scientific Publishing Company: Singapore, 2005.
(2) Li, D.; Xia, Y. *Adv. Mater.* **2004**, *16*, 1151.
(3) Ramakrishna, S.; Fujihara, K.; Teo, W. E.; Yong, T.; Ma, Z.; Ramaseshan, R. *Mater. Today* **2006**, *9*, 40.
(4) Greiner, A.; Wendorff, J. *Angew.Chem., Int. Ed.* **2007**, *46*, 5670.
(5) Kriegel, C.; Kit, K. M.; McClements, D. J.; Weiss, J. *Langmuir* **2009**, *25*, 1154.
(6) Lim, H. S.; Park, S. H.; Koo, S. H.; Kwark, Y. J.; Thomas, E. L.; Jeong, Y.; Cho, J. H. *Langmuir* **2010**, *26*, 19159.
(7) Wang, C.; Hsu, C.-H.; Lin, J.-H. *Macromolecules* **2006**, *39*, 7662.
(8) Shenoy, S.; Bates, W.; Frisch, H.; Wnek, G. *Polymer* **2005**, *46*, 3372.
(9) Cashion, M. P.; Li, X.; Geng, Y.; Hunley, M. T.; Long, T. E. *Langmuir* **2010**, *26*, 678.
(10) McKee, M.; Layman, J.; Cashion, M.; Long, T. *Science* **2006**, *311*, 353.
(11) Celebioglu, A.; Uyar, T. *Chem. Commun.* **2010**, *46*, 6903.
(12) Szente, L.; Szejtli, J.; Kis, G. *J. Pharm. Sci.* **1998**, *87*, 778.
(13) Bonini, M.; Rossi, S.; Karlsson, G.; Almgren, M.; Nostro, L. P.; Baglioni, P. *Langmuir* **2006**, *22*, 1478.
(14) Messner, M.; Kurkov, S.; Jansook, P.; Loftsson, T. *Int. J. Pharm.* **2009**, *387*, 199.
(15) Hedges, A. R. *Chem. Rev.* **1998**, *98*, 2035.
(16) Szejtli, J. *Chem. Rev.* **1998**, *98*, 1743.
(17) Samperio, C.; Boyer, R.; Eigel, W. N.; Holland, K. W.; McKinney, J. S.; O'Keefe, S. F.; Smith, R.; Marcy, J. E. *J. Agric. Food Chem.* **2010**, *58*, 12950.
(18) Xu, M.; Wu, S.; Zeng, F.; Yu, C. *Langmuir* **2010**, *26*, 4529.
(19) Park, I. K.; von Recum, H. A.; Jiang, S.; Pun, S. H. *Langmuir* **2006**, *22*, 8478.
(20) Uyar, T.; Havelund, R.; Hacaloglu, J.; Besenbacher, F.; Kingshott, P. *ACS Nano* **2010**, *4*, 5121.
(21) Uyar, T.; Havelund, R.; Hacaloglu, J.; Zhou, X.; Besenbacher, F.; Kingshott, P. *Nanotechnology* **2009**, *20*, 125605.
(22) Uyar, T.; Balan, A.; Toppare, L.; Besenbacher, F. *Polymer* **2009**, *50*, 475.
(23) Uyar, T.; Nur, Y.; Hacaloglu, J.; Besenbacher, F. *Nanotechnology* **2009**, *20*, 125703.
(24) Uyar, T.; Hacaloglu, J.; Besenbacher, F. *React. Funct. Polym.* **2009**, *69*, 145.
(25) Uyar, T.; Kingshott, P.; Besenbacher, F. *Angew. Chem., Int. Ed.* **2008**, *47*, 9108.
(26) Coleman, A. W.; Nicolis, I.; Keller, N.; Dalbiez, J. P. *J. Inclusion Phenom. Macrocyclic Chem.* **1992**, *13*, 139.
(27) Hausler, O.; Muller-Goymann, C. C. *Starch/Staerke* **1993**, *45*, 183.
(28) Uyar, T.; Besenbacher, F. *Polymer* **2008**, *49*, 5336.
(29) Hinze, W.; Pharr, D. Y.; Fu, Z. S.; Burkert, W. G. *Anal. Chem.* **1989**, *61*, 422.
(30) González-Gaitano, G.; Rodríguez, P.; Isasi, J. R.; Fuentes, M.; Tardajos, G.; Sánchez, M. *J. Inclusion Phenom. Macrocyclic Chem.* **2002**, *44*, 101.
(31) Paulidou, A.; Maffeo, D.; Yannakopoulou, K.; Mavridis, I. M. *Carbohyd. Res.* **2008**, *343*, 2634.
(32) Jug, M.; Kosalec, I.; Maestrelli, F.; Mura, P. *J. Pharm. Biomed.* **2011**, *54*, 1030.
(33) Duan, M. S.; Zhao, N.; Ossurardottir, I. B.; Thorsteinsson, T.; Loftsson, T. *Int. J. Pharm.* **2005**, *297*, 213.
(34) Qiu, X. M.; Sun, D. Z.; Wei, X. L.; Yin, B. L. *J. Solution Chem.* **2007**, *36*, 303.
(35) Othman, M.; Bouchemal, K.; Couvreur, P.; Gref, R. *Int. J. Pharm.* **2009**, *379*, 218.
(36) Harada, A.; Li, J.; Kamachi, M. *Macromolecules* **1993**, *26*, 5698.
(37) Becheri, A.; Nostro, P. L.; Ninham, B. W.; Baglioni, P. *J. Phys. Chem. B* **2003**, *107*, 3979.
(38) Guan, Y.; Qian, L.; Xiao, H. *Macromol. Rapid Commun.* **2007**, *28*, 2244.
(39) Koontz, J. L.; Marcy, J. E.; O'keefe, S. F.; Duncan, S. E. *J. Agric. Food Chem.* **2009**, *57*, 1162.
(40) Giordano, F.; Novak, C.; Moyano, J. R. *Thermochim. Acta* **2001**, *380*, 123.
(41) Uyar, T.; Hunt, M. A.; Gracz, H. S.; Tonelli, A. E. *Cryst. Growth Des.* **2006**, *6*, 1113.
(42) Sigurdsson, H. H.; Knudsen, E.; Loftsson, T.; Leeves, N.; Sigurjonsdottir, J. F.; Másson, M. *J. Inclusion Phenom. Macrocyclic Chem.* **2002**, *44*, 169.